

The use of the EGS4 simulation code to evaluate the response of NaI(Tl) detector for photons in the energy range <300 keV

FAYEZ H. H. AL-GHORABIE

*Department of Physics, Faculty of Applied Sciences,
Umm Al-Qura University, P. O. Box 10130,
Makkah, Saudi Arabia*

EGS4

EGS4

(NaI-RESPO)

NaI(Tl)

K

In this paper the EGS4 simulation code was used to study the response of NaI(Tl) detector when exposed to gamma rays photons in the energy range <300 keV. The study included the recording of incident rays spectra and photopeak determination. In addition the probability of K X-ray escape from a NaI(Tl) crystal and its dependence on detector shape and volume was considered. The obtained results showed an excellent agreement between the theoretical calculations and the experimental results which indicate the high efficiency of the used simulation code to quantify physical parameters that are difficult to evaluate by experimental methods.

Key words: X-rays, EGS4 simulation code, NaI(Tl) detector.

INTRODUCTION

The determination of the characteristic response of a scintillation detector to incident gamma photons is a necessary prerequisite to any subsequent quantitative analysis of measured spectra. Although response distributions may be experimentally measured at certain energies using monoenergetic nuclide sources,

the number of such sources is quite limited. In order to obtain response at energies intermediate to those of the nuclides, i.e., as a function of energy, the researcher must resort to either a complicated interpolation of the limited experimental spectra or to a calculation of distributions using the Monte Carlo method (Zerby & Moran 1962; Weitkamp 1963; Giannini *et al.* 1970).

The aim of this study is to calculate the accurate response for low energy gamma rays below 300 keV. For this purpose, a user-code (NaI-RESPO) based on the use of the EGS4 Monte Carlo code (Ford & Nelson 1978; Nelson *et al.* 1985; Nelson & Rogers 1988) was developed. This user-code considers the processes subsequent to photoelectric absorption, that is, the emission of a fluorescent X-ray or an Auger electron. In the photoelectric absorption process, a characteristic X-ray is emitted by the absorber atom. In the majority of cases this X-ray energy is reabsorbed fairly near the original interaction site. If the photoelectric absorption occurs near a surface of the detector, however, the X-ray photon may escape. In this event, the energy deposited in the detector is decreased by an amount equal to the X-ray photon energy. Without the X-ray escape, the original gamma ray would have been fully absorbed and the resulting pulse would have contributed to the photopeak. With escape, a new category of events is created in which an amount of energy equal to the original gamma ray energy minus the characteristic X-ray energy is repeatedly deposited in the detector. Therefore, a new peak will appear in the response function and will be located at a distance equal to the energy of the characteristic X-ray below the photopeak. These peaks are generally labeled "X-ray escape peaks" and tend to be most prominent at low incident gamma ray energies and for detectors whose surface-to-volume ratio is large (Knoll 1989). Fig. 1 shows the response function of a NaI(Tl) detector following incidence of gamma rays. Though there have been some calculations which take the K X-ray escape into account (Giannini *et al.* 1970), yet the effect of the K X-ray escape on the response functions has not been fully described.

In the present work, a treatment of the processes subsequent to the photoelectric effect will be described. Next, the calculated response is compared with the experimental one, the K X-ray escape from a NaI (Tl) crystal and the non-linear response of the detector to gamma ray energy (which is prominent at low energy) are examined. Finally, the change of the response functions is discussed in connection with the incident gamma ray energy.

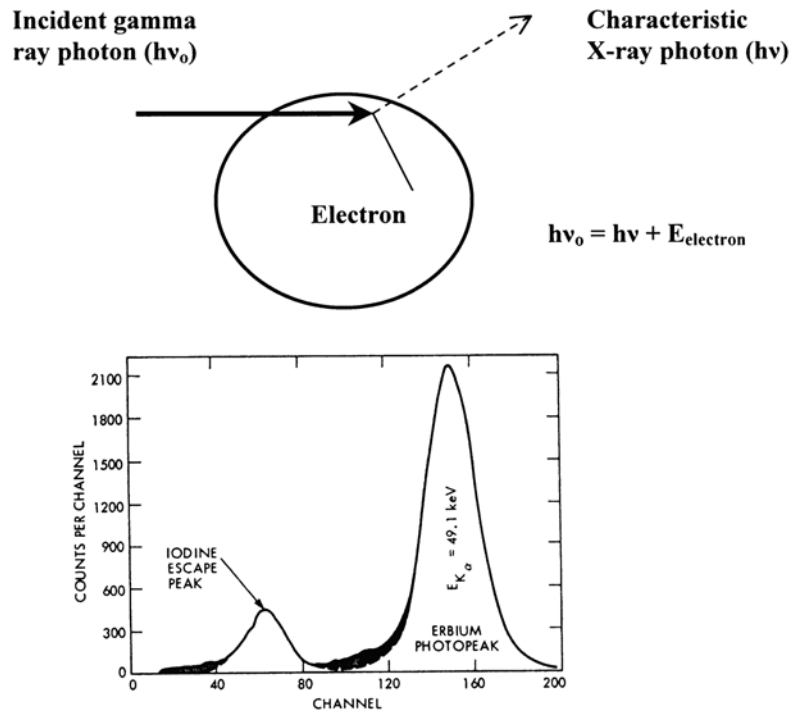


Fig. 1. The processes of photoelectric absorption and X-ray escape is shown at the top. The bottom shows a low-energy spectrum from a NaI(Tl) scintillator for incident 49.1 keV X-rays from Erbium. The Iodine characteristic X-ray escape peak lies 25 keV below the photopeak. (From Knoll 1989)

MATERIALS AND METHODS

The EGS4 code system

The EGS4 code system is a well-structured and thoroughly documented system of programs which allow the user to simulate electromagnetic cascade showers in any material (Ford & Nelson 1978; Nelson *et al.* 1985; Nelson & Rogers 1988). Examples of the usage of this code in the applications of medical radiation physics are given in the literature (Kilic 1995; Lewis *et al.* 1995; Al-Ghorabie 1999; Jeraj *et al.* 1999; Siebers *et al.* 1999; Zaidi 1999; Al-Ghorabie *et al.* 2001). Essentially the user writes:

- (1) a user code which handles input, output and initialization of various parameters.
- (2) a subroutine to specify the geometry of the particular problem.
- (3) a scoring routine which keeps track of the quantities of interest (in this case the energy deposited in the active detector volume).

The EGS4 code system is written in a structured language called Mortran3 (Nelson *et al.* 1985) developed at Stanford Linear Accelerator Centre (SLAC). It is essentially an extension of standard FORTRAN. Although it is possible to program EGS4 entirely in FORTRAN, use of Mortran3 results in very much shorter and more readable code. The EGS4 code is available on the Internet. The latest version can be downloaded free of charge from the web site. *

The user code NaI-RESPO used in this work consists of a main program and several subroutines which use the EGS4 system to simulate energy deposition in the NaI(Tl) detector. In terms of running the code, the major critical parameters are the source geometry, the number of histories to follow and the energy cut-offs to use (the energies below which electrons or photons are deemed to lose all their energy locally). The NaI-RESPO user code is available from the author upon request. The preparation of the data files required for a particular set of materials is handled by a separate program called PEGS. The physical processes considered in this work are briefly reviewed below.

Photoelectric effect

Every photoelectric absorption is supposed to be caused by iodine, because the absorption probability by iodine is much higher than the probability by sodium. It is assumed that a photon with less than the K-shell binding energy is absorbed by removing the L-shell electron, and that a photon with more than the K-shell binding energy can cause both K-shell and L-shell absorption. Though photoelectric absorption by the outer shells is possible, the occurrence probability is extremely low. The ratio of K-shell absorption to the total photoelectric absorption is almost constant, but increases a little as a function of photon energy (Siegbahn 1965). Here, the ratio is assumed to be constant at 0.89. When a K-shell vacancy is filled by an electron coming from the outer shells, a K X-ray or an Auger electron is emitted. The probability of K X-ray emission subsequent to K-shell absorption ω_K , was obtained from the equation according to Burshop (Wapstra *et al.* 1959),

$$\left(\frac{\omega_K}{1 - \omega_K} \right)^{1/4} = -A + BZ - CZ^3 \quad (1)$$

where Z is the atomic number. Using the following $A = 6.4 \times 10^{-2}$, $B = 3.4 \times 10^{-2}$, $C = 1.03 \times 10^{-6}$, ω_K was calculated to be 0.86.

*<http://www.irs.inms.nrc.ca/inms/irs/EGSnrc/EGSnrc.html>

In transitions of electrons coming from the higher shells to the K-shell, the important ones are expressed in the Siegbahn notation as follows:

$$\begin{aligned}
 K_{\alpha 1} &= K - L_{III} \\
 K_{\alpha 2} &= K - L_{II} \\
 K_{\beta 1} &= K - M_{III} \\
 K_{\beta 2} &= K - N_{III} \\
 K_{\beta 3} &= K - M_{II} \\
 K_{\beta 4} &= K - N_{II} \\
 K_{\beta 5} &= K - M_{IV}
 \end{aligned} \tag{2}$$

These transitions were classified into four groups of:

$$\begin{aligned}
 &K_{\alpha 1}, K_{\alpha 2}, K_{\beta_1^-} (= K_{\beta 1} + K_{\beta 3} + K_{\beta 5}) \quad \text{and} \\
 &K_{\beta_2^-} (= K_{\beta 2} + K_{\beta 4} + \text{other transitions}).
 \end{aligned}$$

Table 1 shows the occurrence probability of each transitions and the energy liberated (Wapstra *et al.* 1959). For $K_{\beta_1^-}$ and $K_{\beta_2^-}$ transitions, the emitted X-ray energy is assumed to be constant across their respective emission. X-rays from L-shell absorption and any Auger electrons are assumed to lose all their energy soon after they are generated. A K X-ray is assumed to be emitted in a random direction, and is traced until it degenerates under 10 keV of cut-off energy.

Table 1. Probability of transition from outer shells to K-shells and the energy liberated.

Shell	Electron binding energy (keV)	Transition probability from K-shell	Representative K X-ray energy (keV)
K	33.17		
L _{III}	4.56	1.000	28.61
L _{II}	4.85	0.515	28.32
M _{III}	0.88		
M _{II}	0.93	0.273	32.30
M _{IV}	0.63		
N _{III}	0.12	0.057	33.05
N _{II}	0.12		

Compton scattering

Direction and energy of a photon after Compton scattering are randomly

sampled by making use of the Klein-Nishina formula. At low energy, the scattering angle distribution of a photon differs from the Klein-Nishina law, since the binding between an electron and a nucleus perturbs the scattering. Nevertheless, the photoelectric effect occurs so frequently that the perturbation is expected to make little change in calculation. Here, the Compton scattering features are decided in accordance with the Klein-Nishina formula.

Experimental measurement of detector response function

In the present work the response function of a 2"×2" NaI(Tl) cylindrical scintillation detector was measured experimentally. Fig. 2 shows a schematic diagram of the experimental set-up.

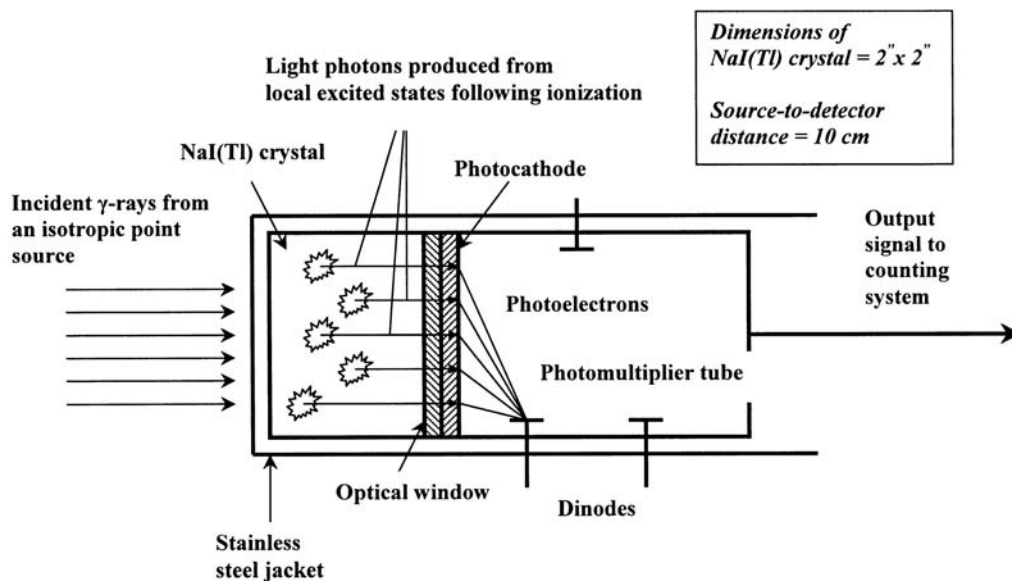


Fig. 2. A schematic diagram of the experimental set-up.

An ^{241}Am source was located at a distance of 10 cm on the axis of the NaI(Tl) detector. The NaI (Tl) crystal is sealed in a stainless steel jacket with a transparent glass (optical window) at one end to permit the exit of scintillation light from the crystal to the photomultiplier tube. The crystal and photomultiplier tube are sealed in a light-tight jacket to keep out moisture and extraneous light and for mechanical protection. The properties and features of the NaI(Tl) detector used in the experiment are given in Table 2.

Table 2. Properties and features of the NaI(Tl) detector used in the present work.

1	Density (g/cm ³)	3.67
2	Atomic numbers	11, 53
3	Effective atomic number	50
4	Scintillation decay time (nsec)	230
5	Photon yield (per keV)	40
6	Index of refraction	1.85
7	Wavelength of maximum emission (Å°)	4150
8	Dimensions	2 in. dia. x 2 in. thick
9	Brand	Victoreen
10	Model number	489-120

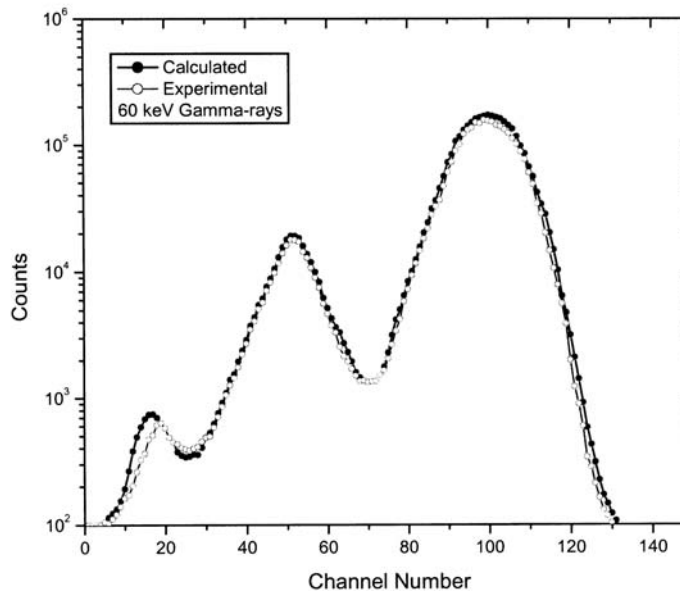
In the experiment, extreme attention was paid to the reduction of photons scattered by surrounding materials other than the detector assembly. This was achieved by performing the experimental measurements in the middle of a large empty laboratory.

RESULTS AND DISCUSSION

Comparison of NaI-RESPO calculations with experiment

A calculated response function using the NaI-RESPO user code was compared with an experimental gamma ray pulse-height spectrum. The comparison in Fig. 3 indicates good agreement between calculation and experiment. To the right of the spectrum, a total-absorbed peak is shown, next an escape peak, and on the left a small compton edge is visible.

Fig. 3. Comparison of calculated and experimental gamma ray response functions for a 2"×2" cylindrical NaI(Tl) detector. A ²⁴¹Am source was located at a distance of 10 cm on the detector axis.



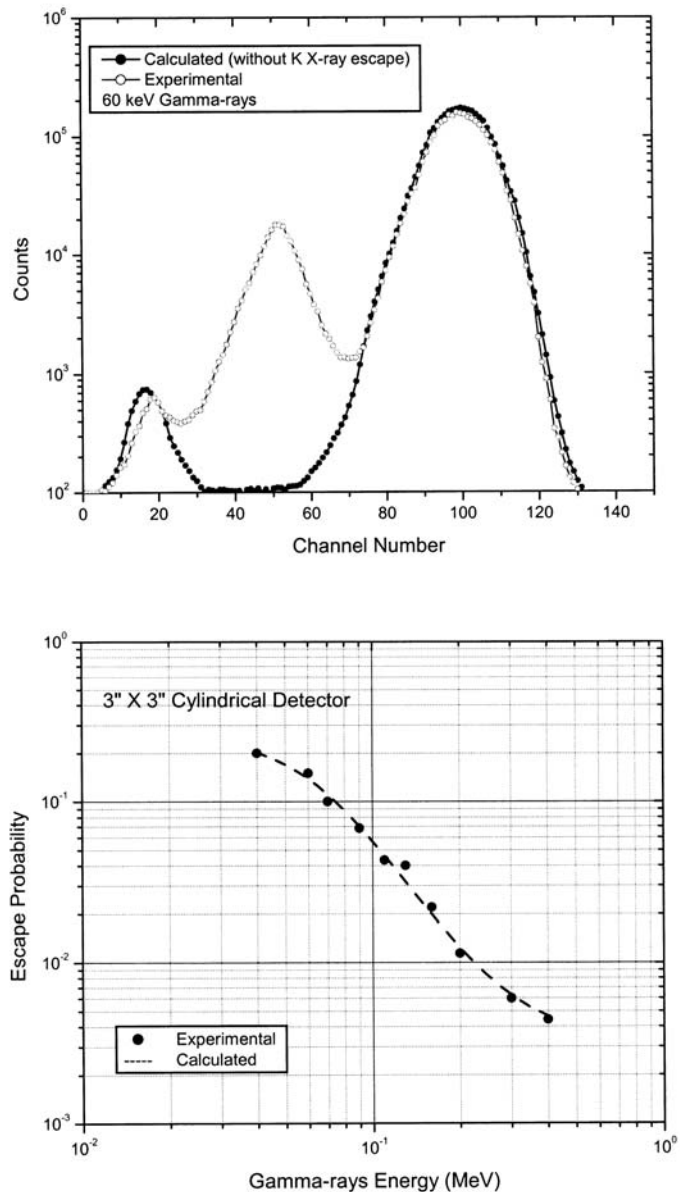
A calculation without consideration of K X-ray escape is compared with the experimental data in Fig. 4. It is clearly shown that K X-ray escape must be included in the low energy response calculation, judging from the large discrepancy observed at the X-ray escape peak.

Fig. 4. Calculated response function without consideration of K X-ray escape. The calculated result is compared with the same experiment as in Fig. 3.

Escape probability of a K X-ray

In the present program, the incidence of photoelectric absorption and K X-ray escape from a NaI(Tl) crystal are recorded, so the escape probability can be easily obtained. Two kinds of response functions were calculated, one is for a parallel beam and another is for a point source at a distance of 10 cm. Since there was no significant difference in escape probability between the two cases, the calculated results for parallel beam are discussed in this section except in connection with Fig. 5. It was found that the calculated K X-ray escape probability is in good agreement with the experimental data of Heath (1964).

Fig. 5. Comparison of Calculated K X-ray probability with experimental data of Heath (1964). A point source was located at a distance of 10 cm on the detector axis.



The relation of the escape probability to the detector shape and volume was examined. Fig. 6 shows the escape probability of cylindrical NaI(Tl) detectors having different volumes.

Fig. 6. K X-ray escape probability of cylindrical NaI(Tl) detectors having different volumes.

The same kind of results for spherical detectors is given in Fig. 7. Less than 100 keV the probability was found to be almost independent of detector volume. Over 100 keV, X-rays generated in a small crystal tend to escape with more frequency than X-rays in a larger crystal. The phenomenon is thought to be due to the X-ray escape through the side surface of the detectors, for incident gamma rays penetrate deep into a NaI(Tl) crystal as the energy increases and the attenuation coefficient decreases.

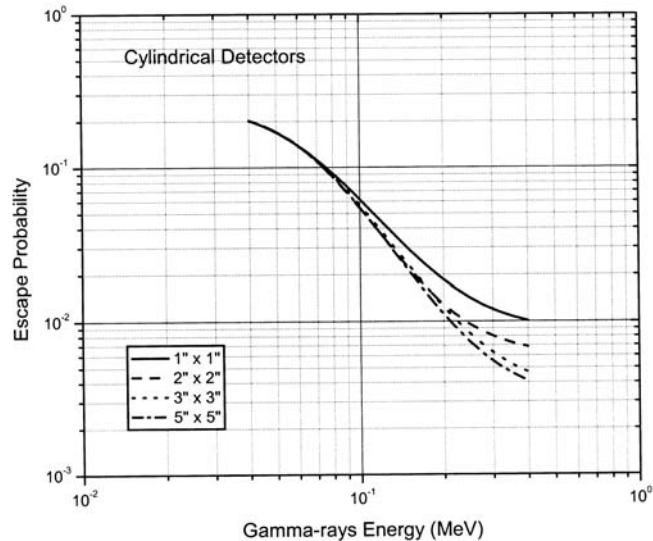


Fig. 7. K X-rays escape probability of spherical NaI(Tl) detectors having different volumes.

Fig. 8 gives the comparison of K X-ray escape probability between a cylindrical detector and a spherical detector. It is clear that K X-rays more easily escape from a spherical detector, at low energies, than from a cylindrical detector by reasons of the convex surface or the dependence on the different ratios between surface and volume for a sphere and a cylinder.

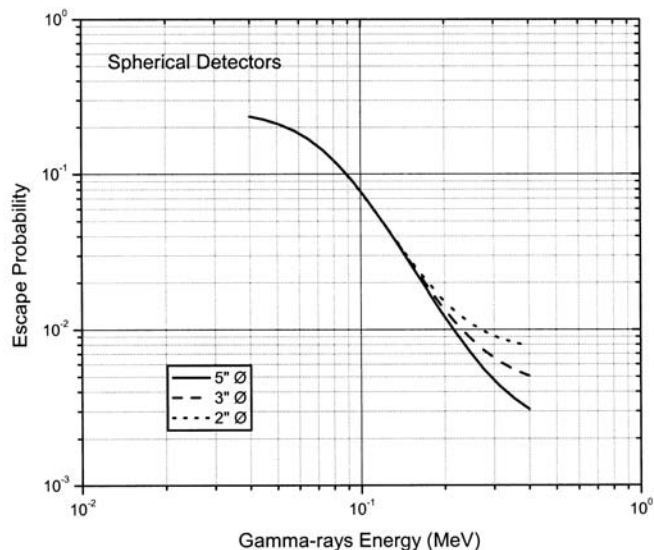
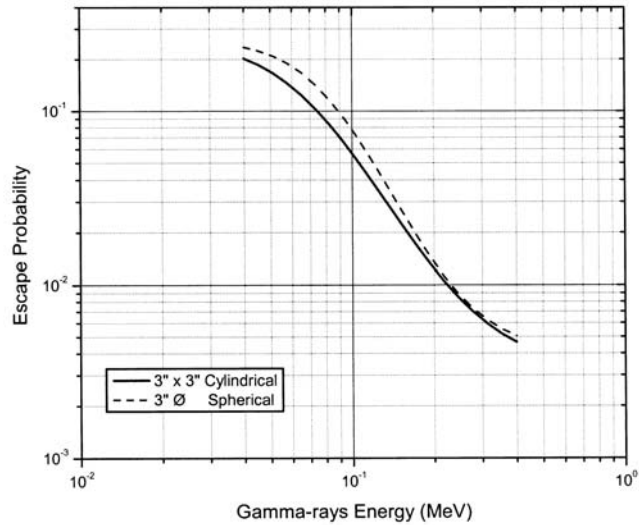


Fig. 8. Comparison of K X-ray escape probability between a 3"Ø spherical NaI(Tl) detector and a 3"×3" cylindrical NaI(Tl) detector.



Variation of response function

The variation of response functions is demonstrated as a function of incident gamma ray energy in Fig. 9. A 3"×3" cylindrical detector was selected by reason of the wide use, and the response functions were calculated for 10^5 parallel gamma rays in the energy range of 40-300 keV. The circles in the figures show the contribution from gamma rays scattered by the detector housing. In this range, a spectrum consists of a total-absorbed peak, a K X-ray escape peak and a Compton continuum. At extreme low energies around 40 keV, a Compton continuum is hidden entirely in a K X-ray escape peak. When the gamma ray energy exceeds 50 keV, the existence of a Compton continuum becomes more noted as the energy increases. Inversely, an escape peak gets smaller as the gamma ray energy increases, and, for a gamma energy over 165 keV, it is difficult to distinguish an escape peak from a total absorbed peak. A peak similar to an escape peak is observed in response functions of 165 keV to 200 keV. However, it is found from Fig. 9 that the peak is not an escape peak but a backscattered peak due to the detector housing.

CONCLUSION

The specific Monte Carlo user-code (NaI-RESPO) was developed for the calculation of the NaI(Tl) scintillation detector response functions for gamma rays under 300 keV. With consideration of K X-ray escape from a NaI(Tl) crystal, the calculation showed good agreement with experimental data. Also, the dependence of these features upon detector shape and volume was examined. A clear difference in K X-ray probability was observed between cylindrical detectors and spherical detectors, however, the detector size hardly influenced the escape probability. The change of response functions according to the incident gamma ray energy was discussed, and the contents of response functions were made clear.

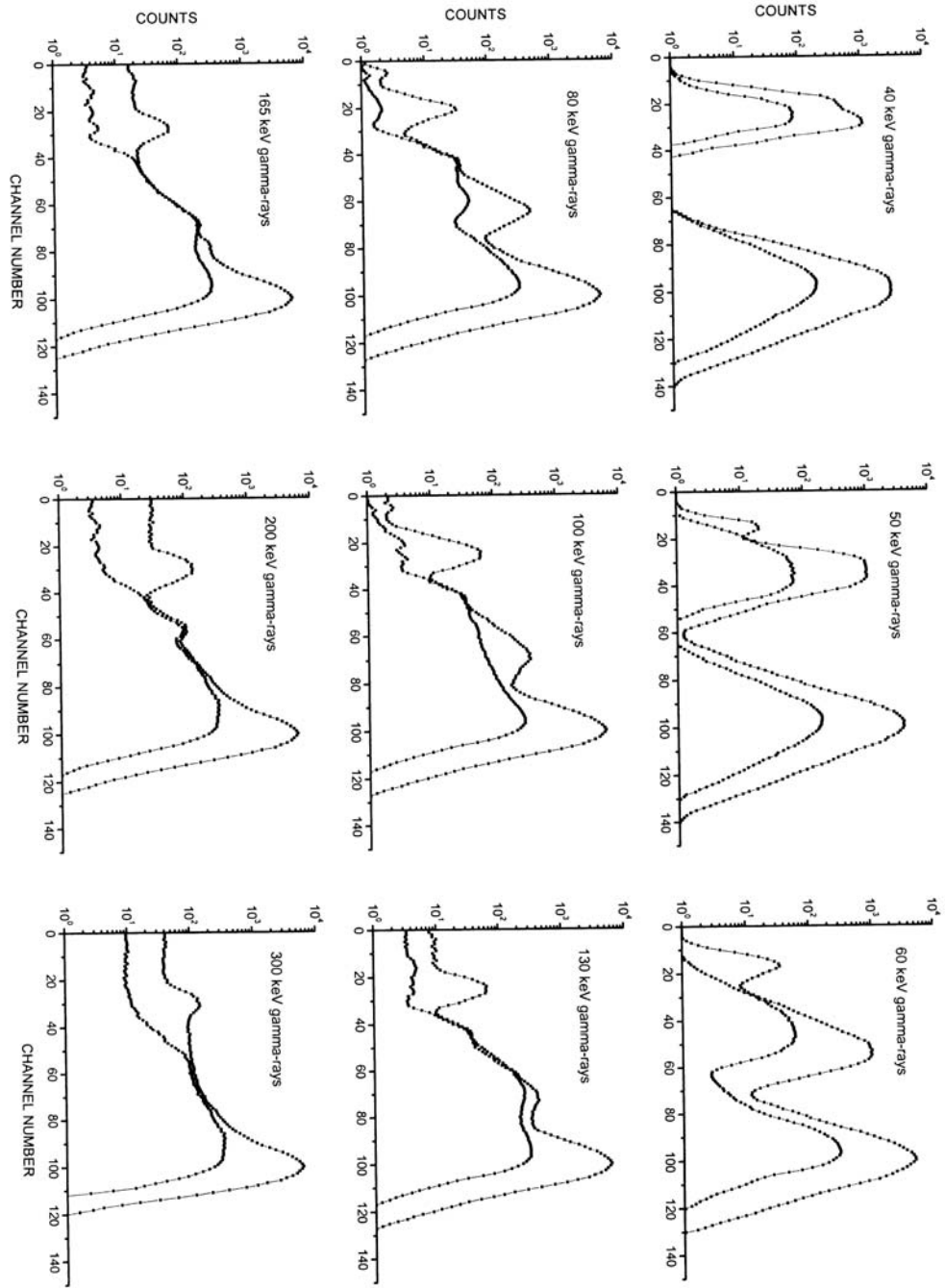


Fig. 9. Change of a gamma ray response function for a 3''x3'' NaI(Tl) detector as a function of energy. Circles stand for the contribution from gamma rays scattered by the detector housing.

ACKNOWLEDGEMENT

I would like to express my deep regards to the referees for valuable suggestions on the manuscript.

REFERENCES

- Al-Ghorabie, F. H. H. 1999.** EGS4 Monte Carlo simulation of a 90° geometry polarized X-ray fluorescence system. *Radiation Physics and Chemistry* 55: 377-384.
- Al-Ghorabie, F. H. H., Natto, S. S. A. & Al-Lyhiani, S. H. A. 2001.** A comparison between EGS4 and MCNP computer modeling of an *in vivo* X-ray fluorescence system. *Computers in Biology and Medicine* 31: 73-83.
- Berger, M. J. & Seltze, S. M. 1972.** Response functions for sodium iodide scintillation detectors. *Nuclear Instruments and Methods in Physics Research* 104: 317-332.
- Ford, R. L. & Nelson, W. R. 1978.** The EGS4 code system: computer programs for the Monte Carlo simulation of electromagnetic cascade showers. Stanford Linear Accelerator Centre Report SLAC-210.
- Giannini, M., Oliva, P. R. & Ramorino, M. C. 1970.** Monte Carlo calculation of The energy loss spectra for gamma rays in cylindrical NaI (TI) crystals. *Nuclear Instruments and Methods in Physics Research* 81: 104-108.
- Heath, R. L. 1964.** Scintillation spectrometry, gamma-ray spectrum catalogue. USAEC Report IDO-16880, USA.
- Jeraj, R., Keall, P. J. & Ostwald, P. M. 1999.** Comparisons between MCNP, EGS4 and experiment for clinical electron beams. *Physics in Medicine and Biology* 44: 705-717.
- Knoll, G. F. 1989.** Radiation detection and measurement. John Wiley and Sons, New York.
- Kilic, A. 1995.** A theoretical and experimental investigation of polarized X-rays for the *in vivo* measurements of heavy metals. Ph.D. thesis, University of Wales, Swansea, UK.

- Lewis, D. G., Kilic, A & Ogg, C. A. 1995.** Adaptation of the EGS4 Monte Carlo code for the design of a polarized source for X-ray fluorescence analysis of platinum and other heavy metals *in vivo*. In: *Advances in X-ray Analysis* (Edited by Predecki, P.K., Keith Bowen, D., Gilfrich, J.V., Goldsmith, C.C., Huang, T.C., Jenkins, R., Cev Noyan, I. & Smith, D.K.), Vol. 38, pp. 579-583. Plenum Publishing Corporation, NY, USA.
- Nelson, W. R., Hirayama, H. & Rogers, D. W. 1985.** The EGS4 code system. Stanford Linear Accelerator Centre Report SLAC-265.
- Nelson, W. R. & Rogers, D. W. 1988.** Structure and operation of the EGS4 code system. In: *Monte Carlo Transport of Electrons and Photons* (Edited by Jenkins, T.M., Nelson, W.R. & Rindi, A.) pp 287-310. Plenum Publishing Corporation, NY, USA.
- Siebers, J. V., Keall, P. J., Libby, B. & Mohan, R. 1999.** Comparison of EGS4 and MCNP4b Monte Carlo codes for generation of photon phase space distributions for a Varian 2100C. *Physics in Medicine and Biology* 44: 3009-3026.
- Siegbahn, K. 1965.** Alpha-, beta- and gamma-ray spectroscopy. North-Holland, Amsterdam.
- Wapstra, A. H., Nijgh, G. J & Van Lieshout, R. 1959.** Nuclear spectroscopy tables. North-Holland, Amsterdam.
- Weitkamp, C. 1963.** Monte Carlo calculation of photofractions and intrinsic efficiencies of cylindrical NaI(Tl) scintillation detectors. *Nuclear Instruments and Methods in Physics Research* 23: 13-18.
- Zaidi, H. 1999.** Relevance of accurate Monte Carlo modeling in nuclear medical imaging. *Medical Physics* 26: 574-608.
- Zerby, C. D. & Moran, H. S. 1962.** Calculation of the pulse-height response of NaI(Tl) scintillation counters. *Nuclear Instruments and Methods in Physics Research* 14: 115-124.